energies

MDPI

Article

Cool Roof Impact on Building Energy Need: The Role of Thermal Insulation with Varying Climate Conditions

Cristina Piselli [1,2], Anna Laura Pisello [1,2], Mohammad Saffari [3], Alvaro de Gracia [2,4,*], Franco Cotana [1,2] and Luisa F. Cabeza [4]

1 Department of Engineering, University of Perugia, 06125 Perugia, Italy
2 CIRIAF-Interuniversity Research Centre, University of Perugia, 06125 Perugia, Italy
3 UCD Energy Institute, University College Dublin (UCD), Belfield, Dublin 4, Ireland
4 GREiA Research Group, INSPIRES Research Centre, University of Lleida, 25001 Lleida, Spain
* Correspondence: adegracia@diei.udl.cat; Tel.: +34-973703333

Received: 25 July 2019; Accepted: 29 August 2019; Published: 30 August 2019

Abstract: Cool roof effectiveness in improving building thermal-energy performance is affected by different variables. In particular, roof insulation level and climate conditions are key parameters influencing cool roofs benefits and whole building energy performance. This work aims at assessing the role of cool roof in the optimum roof configuration, i.e., combination of solar reflectance capability and thermal insulation level, in terms of building energy performance in different climate conditions worldwide. To this aim, coupled dynamic thermal-energy simulation and optimization analysis is carried out. In detail, multi-dimensional optimization of combined building roof thermal insulation and solar reflectance is developed to minimize building annual energy consumption for heating–cooling. Results highlight how a high reflectance roof minimizes annual energy need for a small standard office building in the majority of considered climates. Moreover, building energy performance is more sensitive to roof solar reflectance than thermal insulation level, except for the coldest conditions. Therefore, for the selected building, the optimum roof typology presents high solar reflectance capability (0.8) and no/low insulation level (0.00–0.03 m), except for extremely hot or cold climate zones. Accordingly, this research shows how the classic approach of super-insulated buildings should be reframed for the office case toward truly environmentally friendly buildings.

Keywords: optimization; cool roof; solar reflectance; thermal insulation; energy efficiency in buildings; dynamic simulation

1. Introduction

Nowadays, buildings are responsible for a large part of total energy use and greenhouse gases emissions worldwide [1]. Accordingly, the construction sector has one of the highest potentials for the improvement of sustainable development and global energy efficiency [2]. In fact, almost half of buildings' energy is consumed for thermal performance purposes [3]. Therefore, high-performing building envelopes are needed to meet energy efficient buildings [4]. Taking this into consideration, cool roof technology is a widely acknowledged strategy for building thermal-energy performance improvement, by acting mainly on energy requirement for cooling [5,6] and urban heat island (UHI) phenomenon mitigation [7,8]. Given their high solar reflectance and thermal emissivity properties, indeed, compared to conventional construction materials, cool materials are capable of decreasing the heat released to the outdoor urban environment and to the indoor ambient air [9].

Nevertheless, during the whole year cool roof effectiveness is influenced by different building boundary conditions, including envelope characteristics, end-use, and climate conditions. For instance,

heating energy use penalties in winter may be generated by the implementation of such materials in heating-dominant regions [10,11]. In this view, Hosseini and Akbari [12] focused on cold climates to demonstrate that cool roofs were able to provide annual energy savings in all considered climates for the simulated prototype office and retail buildings. With the aim of estimating the impact of using cool roofs in several climatic conditions, Synnefa et al. [13] simulated the heating and cooling load of residential buildings in 27 cities worldwide. For the case study locations, the cooling load reduction was shown to be higher than the heating penalty. Considering the climate zones of Italy, Costanzo et al. [14] showed that cool roofs can be suitably applied for reducing annual building energy consumption in different Italian cities and with varying insulation levels. However, they highlighted the need to preliminarily evaluate the use of such materials when coupled with very efficient heating systems and high insulation levels in heating-dominant regions. Additionally, Zinzi et al. [15] developed an energy-rating scheme for the application of cool roofs in the Italian climate context for residential buildings according to the results of numerical calculations.

Considering the building envelope design parameters, the roof insulation level is a key element in determining the potential benefits achievable through cool roofs [16]. The effectiveness of cool roofs for the improvement of building indoor thermal comfort conditions was found to be less significant with lower thermal transmittance (U-value) roofing systems [13,17]. On the contrary, Smith et al. [18] stressed that, in temperate climates, standard energy saving approaches, e.g., highly lowering U-value, are unnecessary, unless poor settings are made in other parameters. A further study carried out in hot, arid climate [19] demonstrated that the difference in heat gains through the roof with and without thermal insulation is lower when a cool roof is implemented than with other roof systems. Additionally, Di Giuseppe et al. [20] analyzed the impact of combining different building envelope U-value levels and roof coating optical properties on the UHI in an Italian urban context. The results of fluid-dynamic microclimate simulations showed that the combination of low solar reflectance surfaces, highly insulated envelopes, and lower urban canyons involves increased environment air temperatures.

Given this interaction between roof coating optical properties and sub-roof insulation level for building energy efficiency, optimization analysis involving these two envelope characteristics appears to be a valuable tool. Optimization techniques, indeed, were spreading in the last few years for efficient building design [21]. Both multi-objective and single-objective optimization studies were performed for improving buildings energy performance. For instance, Dávi et al. [22] studied the energy performance and economy of a hybrid photovoltaic system with demand-side management for an office building through multi-objective optimization. Kuang et al. [23] determined the most economical operation schedule of a combined heating, cooling, and power system with energy storage unit. By focusing on the building envelope, Cascone et al. [24] investigated the optimal properties and application of phase change materials for the energy retrofit of the opaque envelope of an office building. As for roof layout optimization, Gentle et al. [25] performed a systematic analysis of the combined effect of three roof parameters, i.e., thermal resistance (R-value), thermal emittance, and solar albedo. Cool roofs were shown to optimize environmental benefits and cost when tailoring the sub-roof R-value to the spectral properties of the roof. Moreover, the energy savings impact due to integrating an additional phase change material (PCM) layer into the roof was assessed [26]. Instead, Farhan et al. [27] developed a building information modelling (BIM) based approach to define the most effective technology able to improve the thermal comfort level of residential buildings while reducing CO_2 emissions. Arumugam et al. [28] optimized the interaction of roof albedo and insulation in different Indian climate zones via energy simulation and parametric analysis. The insulation thickness increase was demonstrated to provide incremental benefits in energy savings which were reduced after a limit. Similarly, Ramamurthy et al. [29,30] studied the joint influence of these two roof characteristics on building energy performance through a two-step experimental and numerical analysis. They highlighted the role of both albedo and insulation thickness for the reduction of the annual energy load attributable to the roof, and that wintertime penalties are negligible compared to summertime benefits with cool roofs. Finally, Saafi and Daouas [31] demonstrated through life-cycle

cost analysis the cost-effectiveness of aged and restored cool roofs for non-insulated roofs in the specific Tunisian climate.

Building upon the existing literature and previous contributions [32–34], the purpose of this study was to assess the effectiveness of designing consistent thermal insulation level and roof solar reflectance capability in terms of annual energy savings of the heating ventilation and air conditioning (HVAC) system in different climate zones in the world. Based on the consolidated knowledge about cool roofs effectiveness as a passive cooling strategy and the key influence of roof R-value on such performance, as demonstrated by the previous study [32] and by various scientific contributions worldwide, this study used a replicable method for improving building thermal-energy behavior by optimizing the roof configuration design. Accordingly, the novelty of this study consisted of analyzing the optimum coupling of roof solar reflectance and insulating layer thickness for minimizing annual air-conditioning energy use for office buildings in selected representative climate zones worldwide. The methodology implemented a replicable and time-saving procedure based on the coupling of dynamic thermal-energy deterministic simulation with optimization analysis, which could be reduplicated in a variety of climate contexts worldwide. Therefore, this study bridged the gap between theory and practice by providing indications for the energy efficient design of building roof coatings in different climates. In this way, outcomes on the effectiveness of cool roofs, usually referred to a specific case study, could be generalized varying several boundary conditions. For instance, guidelines for the effective design of roof layout could be developed based on the considered climate conditions.

2. Methodology

2.1. Overview

Simulation-based optimization is an important and initial step for designing energy-efficient buildings and evaluating innovative green and sustainable strategies [21]. In the present paper, EnergyPlus building simulation software [35] was used to numerically evaluate the building prototypes and then, for optimization purposes, it was coupled with a generic optimization program, i.e., GenOpt [36]. Figure 1 provides a general view of the methodology implemented for the numerical analysis.

Therefore, the methodology was based on numerical analysis via coupled dynamic thermal-energy building simulation and optimization. In detail, the work investigated the optimum roof configuration that minimized annual building energy consumption for air conditioning within different climate zone conditions. The roof coating solar reflectance and thermal insulation layer thickness were selected as the two variables affecting building energy performance. Based on acknowledged literature, the considered values of roof solar reflectance (ρ_{solar}) ranged from 0.1, i.e., dark roof, to 0.8, i.e., cool roof [13,37]. As for roof thermal insulation, standard expanded polystyrene (EPS), i.e., characterized by thermal conductivity equal to 0.04 W/m·K, was used as insulating material. The considered range of thickness ($thickness_{ins}$) varied from 0.00 m, i.e., no roof thermal insulation, to 0.25 m, based on technical knowledge.

For the purpose of the study, various case study weather conditions representing diversified climate zones worldwide were considered. Regarding the case study building, the American Society of Heating, Refrigerating and Air-Conditioning Engineers (ASHRAE) standard model for small office building [38] was used as the case study building. In the validated model, only the envelope components thermal transmittance (U-value) was modified varying the climate zone. First, one-dimensional optimization analysis was implemented when varying the sole roof (i) solar reflectance or (ii) thermal insulation thickness. When focusing on thermal insulation level variation, two different roof solar reflectance scenarios were considered, i.e., "standard roof", where the ρ_{solar} value was left equal the value of the ASHRAE standard model [38], namely 0.3, and "cool roof", where the ρ_{solar} value was set equal to the maximum selected value, namely 0.8. Therefore, building annual energy consumption sensitivity to the variation of these two parameters was assessed to evaluate their separate contribution in

different climate zones. Second, multi-dimensional optimization analysis was carried out to define the optimum roof configuration, i.e., by coupling the characterization of solar reflectance capability and thermal insulation level, to minimize building annual energy use in each considered climate condition. The optimization was run in several cities characterized by different heating degree days (HDD) and, therefore, representing various climate zones worldwide for both one-dimensional and multi-dimensional optimization analysis. The selected climate zones are defined in detail later in Section 2.4.

Finally, a complementary cost analysis was carried out to compare the construction cost of cool roof solutions to the standard construction approach of dark roof with high thermal insulation level. The purpose of this analysis was to evaluate the further cost-effectiveness of the integrated design of the optimum roof configuration.

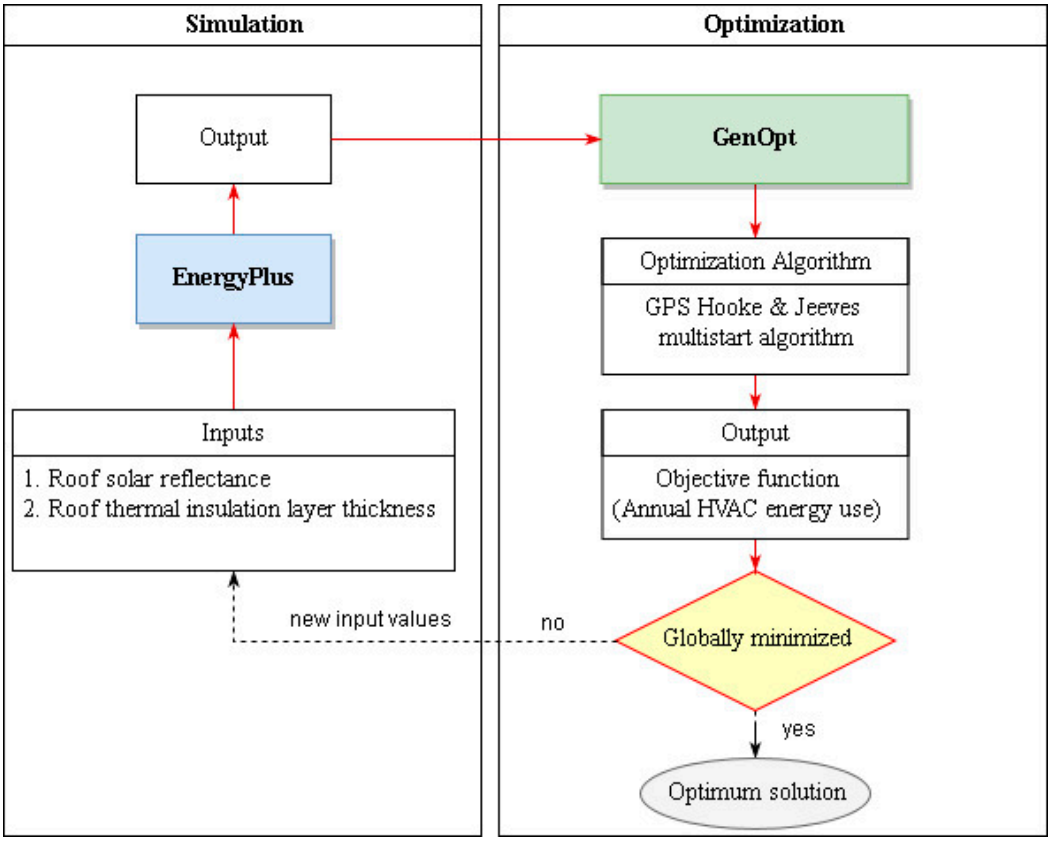

Figure 1. Schematic view of the methodology.

2.2. Numerical Modeling

In accordance with previous contributions using the same methodology [32,33], this study implemented the acknowledged simulation engine EnergyPlus v8.4.0 [35] to develop the dynamic simulations. EnergyPlus is a whole-building thermal-energy dynamic simulation program [39], which includes many advanced modeling tools, such as simulation of materials with variable thermal properties, integrated loads, systems and plant calculations in the same time step, heat balance load calculations, algorithms for analyzing human thermal comfort, etc. Further capabilities that characterize this calculation engine are general envelope calculations (with inside and outside surface convection algorithms) as well as advanced ventilation, infiltration, room air, multi-zone airflow calculations, and fenestration analysis [40]. As for the analysis of surfaces optical properties, EnergyPlus includes a solar radiation model for the calculation of direct normal and diffuse horizontal solar radiation. This model is based on the validated direct/diffuse splitting model by Perez et al. [41,42].

In the present study, the conduction transfer function (CTF) algorithm was identified among the available calculation algorithms to calculate transient heat conduction transfer. Furthermore, the "Full Interior And Exterior With Reflections" input was selected for the definition of solar distribution, to take into account both reflected radiation falling on each internal surface, shadow patterns, and solar radiation reflected by surroundings on external building surfaces [43].

2.3. Optimization Analysis

Optimization techniques are getting more popular for designing and evaluating renewable and sustainable building and energy systems [44]. In a considerable number of studies in the area of smart and sustainable buildings, both single-objective and multi-objective optimization methods have been used for optimization of buildings envelopes [45–47]. In this paper, the generic optimization software GenOpt v3.1.1 (Lawrence Berkeley National Laboratory, CA, USA) [36] was used for single-objective optimization. This tool can be coupled with different dynamic simulation software, including EnergyPlus, to solve building energy performance related optimization problems [32,33].

GenOpt, thanks to its user-friendly interface, allows its users to select the appropriate optimization algorithm among the available optimization algorithms. In more detail, the optimization algorithm is capable of finding the independent variables that provide the optimum performance of a user-specified objective function, such as annual air-conditioning energy consumption, evaluated in this study. The objective function is a dependent variable or relation that has to be minimized or maximized. Therefore, optimization problems developed in GenOpt can be generally described by Equation (1):

$$\min_{x \in X} f(x) \tag{1}$$

where $f : X \rightarrow \mathbf{R}$ is the user-defined objective function that measures the system performance and $x \in X \subset \mathbf{R}^n$ is the set of possible design values defined for each independent variable. For the purpose of this study, the optimization problem involves two design parameters, namely roof solar reflectance capability and thermal insulation thickness, which are selected as independent continuous variables. Therefore, each variable can assume any value on the real line in the set of possible values, i.e., between the defined lower and upper bounds, as represented in Equation (2):

$$X = \left\{ x \in \mathbf{R}^n \middle| l^i \leq x^i \leq u^i, i \in \{1, \ldots, n\} \right\} \tag{2}$$

where $l \in \mathbf{R}^n$ and $u \in \mathbf{R}^n$ are the lower and upper bounds, respectively, for design parameters and $-\infty \leq l^i < u^i \leq \infty$ for $i \in \{1, \ldots, n\}$.

In this case, two different optimization problems were performed. Firstly, one-dimensional optimization analysis was defined to minimize building annual energy consumption for air-conditioning by determining the optimum value for roof solar reflectance capability or thermal insulation level, independently (Equation (3)). Therefore, multi-dimensional optimization analysis was designed to find out the optimum combination of roof thermal insulation and solar reflectance to minimize energy consumption for space cooling, as shown in Equation (4):

$$f(x) = E_{total}\left(x^1\right), \tag{3}$$

$$f(x) = E_{total}\left(x^1, x^2\right). \tag{4}$$

In this paper, the Hooke–Jeeves method, which is also named as pattern search, was utilized for both one- and multi-dimensional optimization analyses. This algorithm is a fully known pattern search method in numerical optimization. To find a suitable coordinate of search, the Hooke–Jeeves algorithm initiates with an explorative move by taking into account a single variable at each time on the single individual coordinate paths in the vicinity of an initial point solution. Following this phase, a sequence of pattern progresses are made to accelerate the search in the path discovered in the explorative search.

Hooke–Jeeves compares each preliminary solution with the best earlier solution [48]. More information is available in Lewis et al. [48]. Generally, these algorithms are effective optimization methods, but might achieve the local optima and not the global optima [49]. Therefore, to decrease the risk of not getting the optimum solution, several initial iterations can be selected together with generalized pattern search (GPS) implementation of the Hooke–Jeeves method [50,51]. Selecting several initial points increases the chance of obtaining the global minimum in case of objective functions with various local minima. Therefore, in the present study, the Hooke–Jeeves algorithm with GPS implementation and various starting points was used for minimization of the cost function [21].

2.4. Case Study

2.4.1. Climate Zones

In this study, a variety of climate conditions worldwide was considered. In more detail, 12 cities representing diverse climate zones according to the international Köppen–Geiger classification [52,53] were considered for simulation, including tropical, arid, continental, and temperate conditions. The case study cities were selected based on the research performed by Synnefa et al. [13] and according to the most recent weather files available in the EnergyPlus weather file database [54] in order to have one city in each identified climate zone and to represent a variety of heating degree days (HDD) conditions.

Further details regarding the climate zones, selected cities, and their corresponding HDD and cooling degree days (CDD) for completeness are presented in Table 1.

Table 1. Selected cities, corresponding climate zones, and heating degree days (HDD) and cooling degree days (CDD) [52].

Zone (Köppen–Geiger)	City	HDD	CDD
Aw: Tropical wet and dry climate	Rio de Janeiro, Brazil	5	488
BWh: Hot desert climate	Abu Dhabi, UEA	31	1981
BSh: Hot semi-arid climate	New Delhi, India	271	1388
BSk: Cold semi-arid climate	Thessaloniki, Greece	1057	244
Cfa: Humid subtropical climate	Sydney, Australia	717	112
Cfb: Temperate oceanic climate	Paris, France	2643	53
Cwb: Subtropical highland climate	Mexico City, Mexico	954	22
Csa: Hot-summer mediterranean climate	Rome, Italy	1415	168
Csb: Warm-summer mediterranean climate	San Francisco, USA	2653	13
Dfa: Hot-summer humid continental climate	Beijing, China	2866	299
Dfb: Warm-summer humid continental climate	Moscow, Russia	4748	22
Dfc: Subarctic climate	Tampere, Finland	4068	9

2.4.2. Case Study Building

For the purpose of this work, the validated ASHRAE standard model for small office building was selected [38] (Figure 2). ASHRAE prototype buildings are developed based on department of energy (DOE) Commercial Reference Building Models [55], covering the majority of the commercial building stock. A single-story building model was selected because of the major influence of roof properties on the floor just below it. Additionally, office buildings are usually suitable for the application of cool roofs [12]. The standard office building model presented a rectangular prism shape with total floor area equal to about 510 m^2 (27.7 m × 18.4 m), 3 m height and aspect ratio equal to 1.5. The construction materials for external walls were wood-frame with external plaster, gypsum board on both sides and intermediate insulating layer. The pitched roof was an attic roof with wood joints, EPS insulation, added to achieve acceptable roof U-value in the different climates, gypsum board as internal coating and asphalt shingles as external coating. However, cool tiles were modeled for the "cool roof" scenario.

The dimension of windows was 1.8 m × 1.5 m and the window-to-wall ratio equal to 24.4% for the south-facing façade, while 19.8% for the other orientations [56].

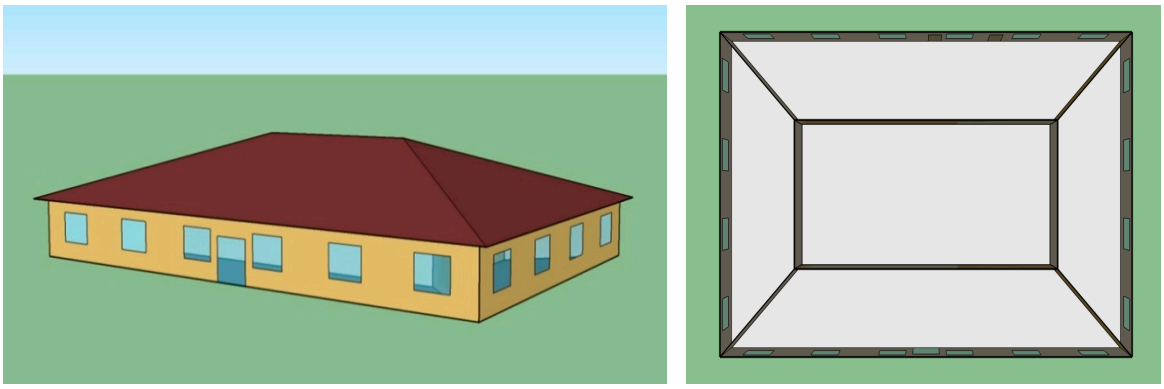

(**a**) (**b**)

Figure 2. Case study ASHRAE standard model for small office building: (**a**) 3D view; (**b**) floor plan perspective view.

To the aim of this study, the main envelope components, i.e., external wall, roof, and windows, of the standard ASHRAE model were adjusted in terms of thermal properties in order to achieve suitable thermal transmittances in each climate zone. In details, values were set in each selected city based on the corresponding HDD and by taking as a reference the general indications of the current building regulation in Italy [57]. In fact, the Italian regulation defines the maximum acceptable U-value for the different components of the external building envelope in a climate zone varying the HDD. In the model, the thermal transmittance values of the main envelope components of the standard model were regulated by modifying the thermal insulation layer thickness in the opaque components or the material and thickness of layers in the windows (when necessary), to get as close as possible to the limit value. The U-values defined for each HDD range are reported in Table 2.

Table 2. Envelope components thermal transmittance (U-values) for the case study small office building model depending on zones HDD.

HDD	U-Value ($W/m^2 \cdot K$)		
	Roof	**External Wall**	**Window**
HDD ≤ 900	0.38 (EPS: 0.09 m)	0.43	3.06
900 < HDD ≤ 1400	0.36 (EPS: 0.10 m)	0.38	2.37
1400 < HDD ≤ 2100	0.30 (EPS: 0.12 m)	0.34	1.93
2100 < HDD ≤ 3000	0.25 (EPS: 0.15 m)	0.30	1.76
HDD ≥ 3000	0.23 (EPS: 0.16 m)	0.28	1.49

Moreover, the specific inputs related to site location and design heating and cooling days were defined in the model according to the EnergyPlus weather files for each climate scenario [54].

2.4.3. HVAC System

The ASHRAE standard building model was served by an air-source heat pump for cooling and for heating in a reverse cycle, and a gas furnace as back up to provide additional heating, when required. The heat pump was auto-sized based on the maximum cooling demand, providing the maximum capacity of the heat pump and the rated coefficient of performance (COP). The distribution of air terminals was one unit per occupied thermal zone considering a constant air volume [58]. According to EN 15251:2007 [59], heating and cooling set-point temperatures were set to 20 °C and 26 °C, respectively. Further on, the minimum and maximum supply air temperatures were set to 13 °C and

40 °C, respectively [38]. Moreover, the case study building was characterized by high internal heat gains, mainly due to lighting and equipment according to the office building typology, i.e., equal to up to 15.6 W/m^2 in the whole building, but variable according to the occupancy schedule [38]. Figure 3 illustrates fan and occupancy schedules of the building model.

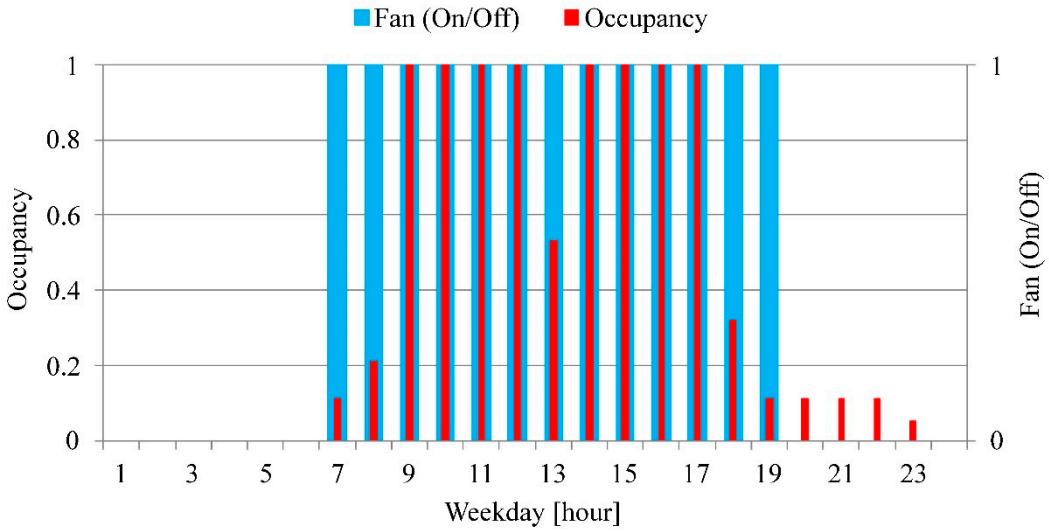

Figure 3. Fan and occupancy schedule of the case study building.

3. Results

3.1. One-Dimensional Roof Solar Reflectance Optimization

The first step of analysis was the one-dimensional optimization of roof solar reflectance in the climate conditions of the 12 selected cities representative of the different climate zones as defined in Table 1. Simulation results in terms of building annual and seasonal, namely total HVAC, cooling, and heating energy use are summarized in Table 3. Results for the standard small office building show that the optimum roof solar reflectance was equal to 0.8, namely it corresponded to the maximum available cool capability, in almost all climates except for the coldest continental and subarctic climate zones of Moscow (Russia) and Tampere (Finland), which were heating dominated climates. Accordingly, the configuration characterized by the worst performance was the dark roof, with ρ_{solar} equal to 0.1 in all climate zones except for the two cities mentioned above. In detail, in the zone characterized anyway by a warm summer humid climate, namely Moscow, an average ρ_{solar} = 0.5 resulted as the optimum value, while in the coldest climate of Tampere the result was inverted involving an optimum roof solar reflectance equal to 0.1. On the other hand, the influence of the variation of roof solar reflectance appeared to be substantial in the hot and warm climates, while it was negligible in the coldest climates.

Furthermore, the sensitivity of building annual energy performance to the variation of roof solar reflectance was evaluated in the different climate zones. Figure 4 presents the trend of total HVAC energy consumption difference (ΔE) between the different scenarios of roof ρ_{solar} in the considered range (0.1–0.8) and the "standard roof" (ρ_{solar} = 0.3) for each case study city. The trend of lines confirmed how the variation of roof solar reflectance was negligible in terms of building annual energy performance in the coldest climates, since the trend was almost flat with energy savings equal to about 132 kWh (3.7%), 118 kWh (1.6%), 17 kWh (0.2%), and 12 kWh (0.1%), in Paris, Beijing, Moscow, and Tampere, respectively, between the optimum and worst ρ_{solar}. On the contrary, in hot and warm climate conditions, which were totally or mainly cooling dominated, the annual HVAC energy need difference for the office building was up to 3.7%, corresponding to about 716 kWh, 3.8% (616 kWh), 3.8% (545 kWh), 7.7% (533 kWh), 5.7% (418 kWh), 4.3% (357 kWh), 5.8% (354 kWh), and 9.5% (284 kWh) in Abu Dhabi, New Delhi, Rio de Janeiro, Mexico City, Sydney, Rome, Thessaloniki, and San Francisco, respectively, between ρ_{solar} equal to 0.8 (optimum) and 0.1 (worst).

Table 3. Heating, cooling, and annual HVAC energy consumption and energy savings with the optimum roof solar reflectance compared to the worst performing scenario for the case study building in each climate zone.

HDD	City	Case	Roof ρ_{solar} (-)	Heating Energy (kWh)	Cooling Energy (kWh)	Annual HVAC Energy (kWh)	Annual HVAC Energy Reduction (%)
5	Rio de Janeiro	Optimum:	0.8	0	13,829	13,829	3.8
		Worst:	0.1	0	14,374	14,374	-
31	Abu Dhabi	Optimum:	0.8	0	18,531	18,531	3.7
		Worst:	0.1	0	19,246	19,246	-
271	New Delhi	Optimum:	0.8	0	15,686	15,686	3.8
		Worst:	0.1	0	16,302	16,302	-
1057	Thessaloniki	Optimum:	0.8	208	5551	5759	5.8
		Worst:	0.1	195	5919	6114	-
717	Sydney	Optimum:	0.8	5	6982	6987	5.7
		Worst:	0.1	5	7400	7405	-
2643	Paris	Optimum:	0.8	1080	2327	3407	3.7
		Worst:	0.1	1039	2500	3539	-
954	Mexico City	Optimum:	0.8	5	6361	6366	7.7
		Worst:	0.1	5	6895	6900	-
1415	Rome	Optimum:	0.8	105	7829	7934	4.3
		Worst:	0.1	104	8187	8291	-
2653	San Francisco	Optimum:	0.8	35	2686	2721	9.5
		Worst:	0.1	33	2971	3004	-
2866	Beijing	Optimum:	0.8	2199	4841	7040	1.6
		Worst:	0.1	2076	5082	7158	-
4748	Moscow	Optimum:	0.5	7755	2129	9884	0.2
		Worst:	0.6	7795	2106	9901	-
4068	Tampere	Optimum:	0.1	7478	1465	8943	0.1
		Worst:	0.8	7619	1335	8954	-

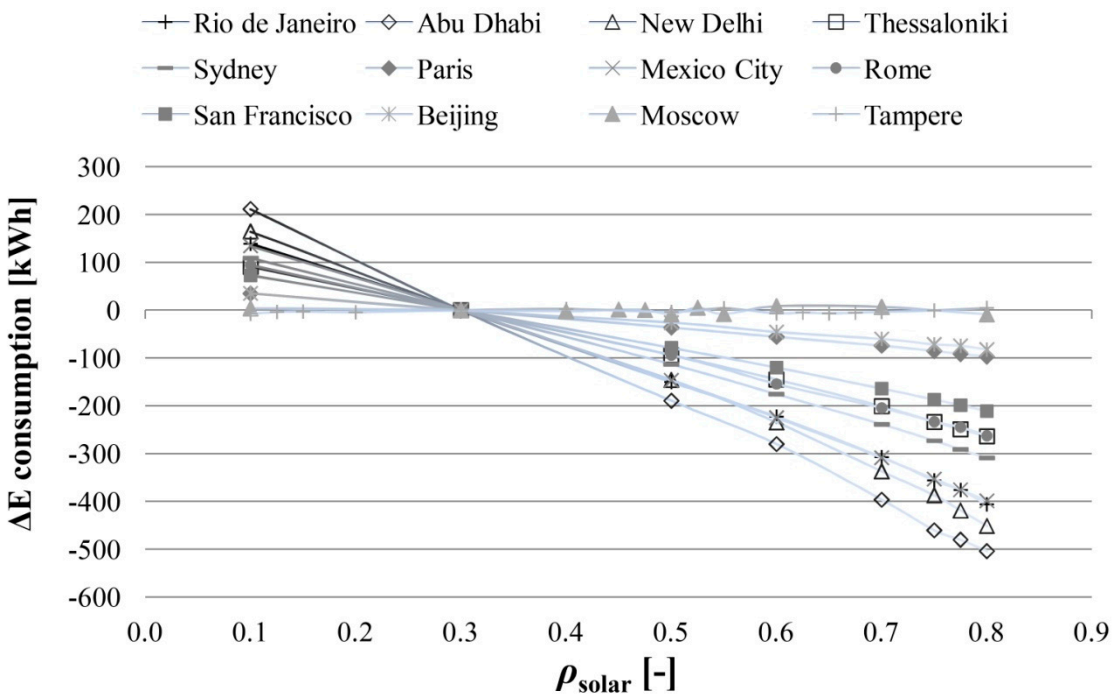

Figure 4. Variation of the annual building HVAC energy consumption difference compared to the standard scenario varying only roof solar reflectance in each climate zone.

3.2. One-Dimensional Roof Thermal Insulation Level Optimization

The same one-dimensional optimization method was applied to analyze the impact of roof thermal insulation on the energy performance of the office building in the case study climate zones by varying only the roof thermal insulation level. In this case, two scenarios were considered for the roof solar reflectance, i.e., (i) "standard roof" and (ii) "cool roof", as previously described.

Concerning the scenario with "standard roof", i.e., ρ_{solar} equal to 0.3, the optimum roof thermal insulation thickness in all considered climates was found to be the maximum available value of 0.25 m (Table 4). However, the effect of insulation level variation was mainly perceived in extreme hot and cold climate conditions, namely in Abu Dhabi, New Delhi, Rio de Janeiro, Moscow, and Tampere. In fact, Figure 5, which reports the trend of total energy consumption difference between the different scenarios of roof $thickness_{ins}$ in the considered range (0.00–0.25) and the "standard roof" ($thickness_{ins}$ according to HDD) for each case study city, depicts higher sensitivity to the variation of thermal insulation in the above-mentioned climate zones. In Abu Dhabi and Tampere, which were in the hottest and coldest climate zone, respectively, the annual HVAC energy savings in the case study building was equal to 3.8% (about 743 kWh) and 6.4% (609 kWh), respectively, between the scenario with the optimum (0.25 m) and the worst (0.00 m) $thickness_{ins}$. Conversely, in milder climates, especially those cooling dominated, the building annual HVAC energy need was only reduced by 200–300 kWh, equal to 2.5%, 3.5%, 4.4%, 4.8%, 6.5%, and 7.4% in Rome, Sydney, Mexico City, Thessaloniki, Paris, and San Francisco, respectively, with the optimum vs. the worst $thickness_{ins}$.

Table 4. Heating, cooling, and annual HVAC energy consumption and energy savings with the optimum roof thermal insulation thickness compared to the worst performing for the case study building with "standard roof" in each climate zone.

HDD	City	Case	Roof $thickness_{ins}$ (m)	Heating Energy (kWh)	Cooling Energy (kWh)	Annual HVAC Energy (kWh)	Annual HVAC Energy Reduction (%)
5	Rio de Janeiro	Optimum:	0.25	0	14,081	14,081	3.5
		Worst:	0.00	0	14,586	14,586	-
31	Abu Dhabi	Optimum:	0.25	0	18,821	18,821	3.8
		Worst:	0.00	0	19,563	19,563	-
271	New Delhi	Optimum:	0.25	0	15,958	15,958	3.8
		Worst:	0.00	0	16,593	16,593	-
1057	Thessaloniki	Optimum:	0.25	193	5768	5961	4.8
		Worst:	0.00	208	6050	6258	-
717	Sydney	Optimum:	0.25	5	7224	7229	3.5
		Worst:	0.00	5	7485	7490	-
2643	Paris	Optimum:	0.25	1029	2442	3471	6.5
		Worst:	0.00	1138	2576	3714	-
954	Mexico City	Optimum:	0.25	5	6682	6687	4.4
		Worst:	0.00	5	6991	6996	-
1415	Rome	Optimum:	0.25	104	8062	8166	2.5
		Worst:	0.00	105	8268	8373	-
2653	San Francisco	Optimum:	0.25	33	2875	2908	7.4
		Worst:	0.00	34	3105	3139	-
2866	Beijing	Optimum:	0.25	2079	4990	7069	5.3
		Worst:	0.00	2241	5222	7463	-
4748	Moscow	Optimum:	0.25	7642	2162	9804	5.9
		Worst:	0.00	8136	2287	10,423	-
4068	Tampere	Optimum:	0.25	7433	1423	8856	6.4
		Worst:	0.00	7951	1514	9465	-

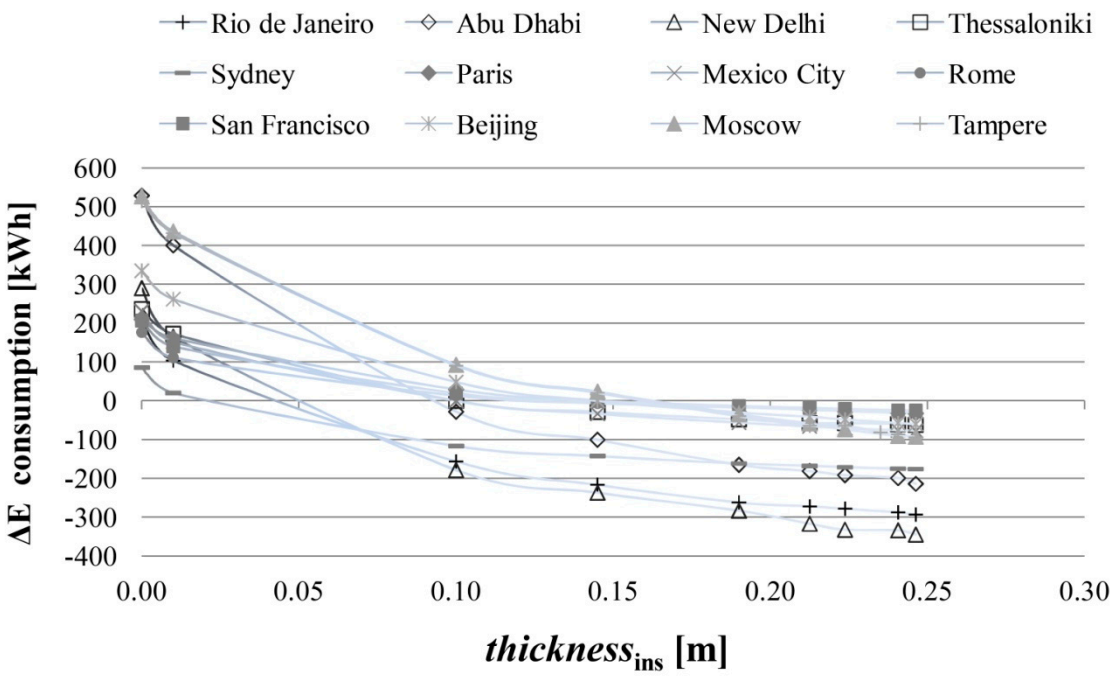

Figure 5. Variation of the annual building HVAC energy consumption difference compared to the standard scenario varying only roof thermal insulation thickness in each climate zone with "standard roof".

On the contrary, in the scenario with "cool roof", i.e., ρ_{solar} equal to 0.8, the maximum available level of thermal insulation, i.e., 0.25 m, minimized annual building HVAC energy consumption only in the coldest climate zones, namely Paris, Beijing, Moscow, and Tampere (Table 5). Accordingly, in these contexts the worst performing configuration was without thermal insulation ($thickness_{ins}$ equal to 0.00 m), due to severe outdoor conditions in winter. On the other hand, in temperate and mild climates, i.e., Sydney, Mexico City, Rome, and San Francisco, the optimum configuration was without thermal insulation (0.00 m) within the roof stratigraphy. In fact, in the considered boundary conditions, high internal heat gains and mild outdoor conditions made the insulation layer disadvantageous in summer and negligible in winter. Finally, in the hottest conditions, i.e., New Delhi, Abu Dhabi, Rio de Janeiro, and Thessaloniki, the optimum was slightly increased up to 0.09 m, 0.04 m, and 0.03 m, respectively. Moreover, the trend of annual energy need difference (compared to the scenario with standard $thickness_{ins}$) was flatter in hot and mild climate zones (Figure 6) and the roof thermal insulation optimization was less significant. In fact, the cooling load, which was predominant in these climate contexts, was minimized by the operation of the high reflectivity coating. Accordingly, up to 72 kWh of total energy saving was achieved in hottest climates, corresponding to only 1.2% in Thessaloniki, and up to 207 kWh benefit was observed in mild climates, corresponding to 2.6% in Rome, between the optimum and worst $thickness_{ins}$. In contrast, in coldest climates, the HVAC energy consumption reduction increased up to 6.8%, corresponding to about 643 kWh in Tampere, between $thickness_{ins}$ equal to 0.25 m (optimum) and 0.00 m (worst).

In general, the one-dimensional optimization analyses showed how the annual HVAC energy consumption of the case study office building was more sensitive to the variation of roof solar reflectance than thermal insulation level, in the considered climate zones, except in the coldest heating dominated conditions.

Table 5. Heating, cooling, and annual HVAC energy consumption and energy savings with the optimum roof thermal insulation thickness compared to the worst performing for the case study building with "cool roof" in each climate zone.

HDD	City	Case	Roof $thickness_{ins}$ (m)	Heating Energy (kWh)	Cooling Energy (kWh)	Annual HVAC Energy (kWh)	Annual HVAC Energy Reduction (%)
5	Rio de Janeiro	Optimum:	0.03	0	13,817	13,817	0.4
		Worst:	0.19	0	13,859	13,859	-
31	Abu Dhabi	Optimum:	0.04	0	18,512	18,512	0.2
		Worst:	0.01	0	18,554	18,554	-
271	New Delhi	Optimum:	0.09	0	15,685	15,685	0.2
		Worst:	0.19	0	15,710	15,710	-
1057	Thessaloniki	Optimum:	0.03	221	5502	5723	1.2
		Worst:	0.19	201	5594	5795	-
717	Sydney	Optimum:	0.00	5	6875	6880	2.3
		Worst:	0.19	5	6951	6956	-
2643	Paris	Optimum:	0.25	1050	2350	3401	2.1
		Worst:	0.00	1225	2249	3474	-
954	Mexico City	Optimum:	0.00	5	6221	6226	3.1
		Worst:	0.19	5	6420	6425	-
1415	Rome	Optimum:	0.00	107	7669	7776	2.6
		Worst:	0.20	105	7879	7984	-
2653	San Francisco	Optimum:	0.00	42	2551	2593	5.3
		Worst:	0.19	34	2702	2736	-
2866	Beijing	Optimum:	0.25	2144	4864	7008	3.5
		Worst:	0.00	2486	4777	7263	-
4748	Moscow	Optimum:	0.25	7736	2071	9807	5.9
		Worst:	0.00	8451	1974	10,425	-
4068	Tampere	Optimum:	0.25	7509	1350	8859	6.8
		Worst:	0.00	8239	1262	9501	-

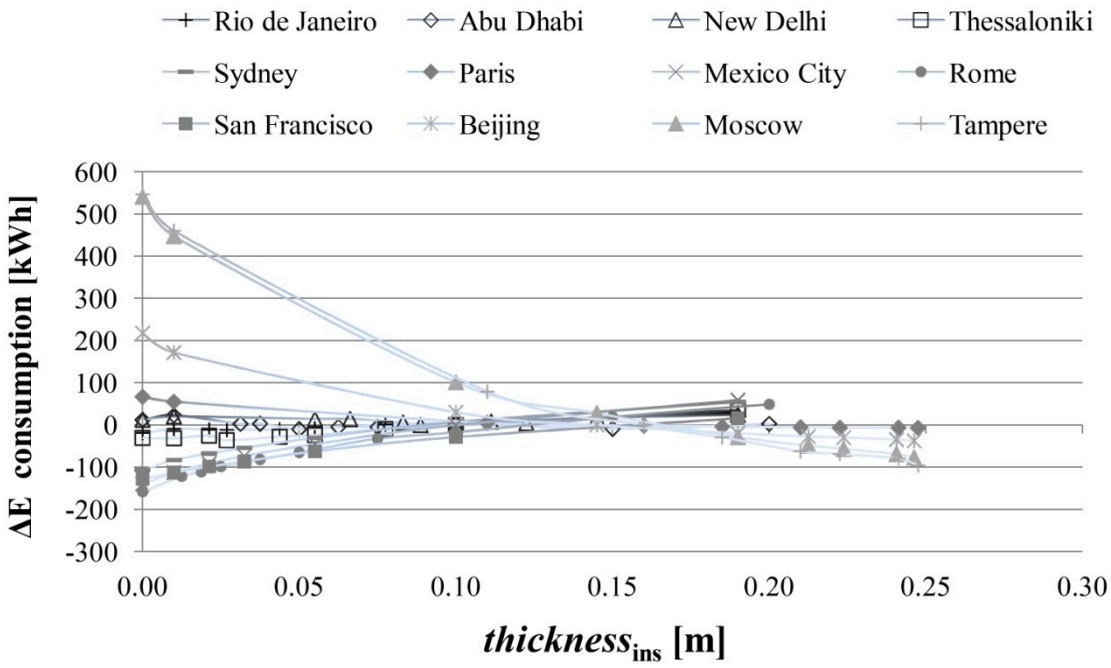

Figure 6. Variation of the annual building HVAC energy consumption difference compared to the standard scenario with varying only roof thermal insulation thickness in each climate zone with "cool roof".

3.3. Multi-Dimensional Roof Configuration Optimization

Figure 7 and Table 6 report the results of the multi-dimensional optimization analysis for the case study climate zones. In detail, the optimum roof configuration (i.e., combination of ρ_{solar} and $thickness_{ins}$) in each city and the corresponding total, heating, and cooling energy consumption are summarized in Table 6. On one hand, the roof configuration that minimized building annual HVAC energy consumption was characterized by high solar reflectance (ρ_{solar} equal to 0.8) in most of the considered climates, except that in the two coldest and heating dominated cities. On the other hand, the thermal insulation level involved in the optimum configuration was more variable with varying the climate context. In particular, in warm and mild climate zones, $thickness_{ins}$ seemed negligible or almost negligible, since values between 0.00 m and 0.03 m optimize the roof energy performance (highlighted in Table 6). Nevertheless, in the hottest climate zones, a suitable thermal insulation level, between 0.11 m and 0.09 m, was required to reduce heat gains by insulating the indoor environment from the hotter outdoor environment. Finally, in the coldest zones, the maximum available $thickness_{ins}$ equal to 0.25 m was required to minimize heating energy losses through the roof. Accordingly, results show how in the majority of considered climate zones (stressed in Table 6 by the rectangle) the optimum roof configuration capable of minimizing annual building energy consumption involved the combination of high solar reflectance capability and low insulation level.

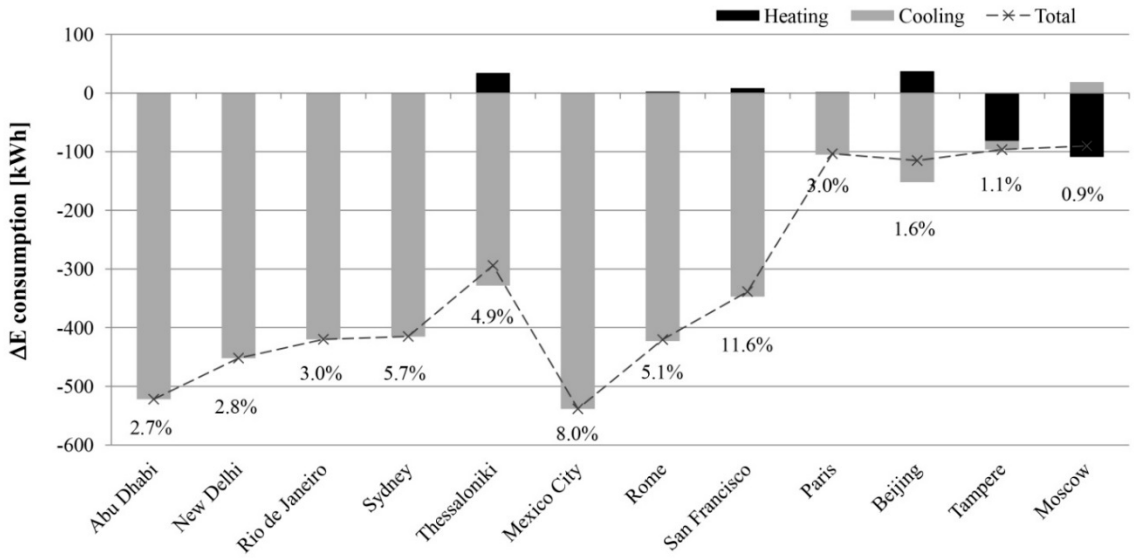

Figure 7. Difference of building HVAC energy consumption between the optimum and the "standard roof" configuration in each climate zone, reporting the annual and the separate contributions for heating and cooling.

Furthermore, Figure 7 illustrates the difference in energy consumption in terms of total and separated heating and cooling energy need between the "standard" (characterized by ρ_{solar} = 0.3 and $thickness_{ins}$ according to the regulation [57] depending on HDD) and the optimum roof configuration in each climate, supported by calibrated dynamic simulation [60]. The comparison between the optimum and the "standard" roof configuration demonstrated how the combined design of roof thermal insulation and solar reflectance generated annual energy savings in all considered climate conditions. However, office building annual HVAC energy consumption was reduced by about 1% to 12% depending on the climate zone. In fact, substantial benefits were mainly perceived in cooling dominated climates. In detail, the maximum achievable actual energy savings were obtained in Mexico City, Abu Dhabi, New Delhi, Rio de Janeiro, Rome, and Sydney, equal to 538 kWh, 522 kWh, 452 kWh, 420 kWh, 420 kWh, and 415 kWh, respectively. Moreover, the energy saving was always found in terms of cooling energy consumption. Conversely, the energy saving was less than 100 kWh in the coldest Moscow and Tampere and the benefits were in terms of heating energy savings.

Table 6. Heating, cooling, and annual HVAC energy consumption and energy savings with the optimum roof configuration compared to the standard roof for the case study building in each climate.

City	Climate Zone	Optimum ρ_{solar} (-)	Optimum $thickness_{ins}$ (m)	Heating (Optimum Roof) (kWh)	Cooling (Optimum Roof) (kWh)	Annual HVAC (Optimum Roof) (kWh)	Annual HVAC (Standard Roof) (kWh)	Annual HVAC Energy Savings (%)
Abu Dhabi, UEA	BWh	0.8	0.11	0	18,513	18,513	19,035	2.7
New Delhi, India	BSh	0.8	0.09	0	15,685	15,685	16,137	2.8
Rio de Janeiro, Brazil	Aw	0.8	0.03	0	13,815	13,815	14,235	3.0
Thessaloniki, Greece	BSk	0.8	0.00	232	5497	5728	6022	4.9
Sydney, Australia	Cfa	0.8	0.00	5	6875	6880	7295	5.7
Mexico City, Mexico	Cwb	0.8	0.00	5	6221	6226	6765	8.0
Rome, Italy	Csa	0.8	0.00	107	7669	7776	8197	5.1
San Francisco, USA	Csb	0.8	0.00	42	2551	2593	2931	11.6
Paris, France	Cfb	0.8	0.25	1051	2350	3401	3504	3.0
Beijing, China	Dfa	0.8	0.25	2143	4864	7007	7122	1.6
Tampere, Finland	Dfc	0.4	0.25	7437	1416	8853	8949	1.1
Moscow, Russia	Dfb	0.1	0.25	7610	2192	9802	9893	0.9

3.4. Comparative Cost Analysis

To the aim of the comparative cost analysis between the standard dark roof approach and the cool roof solution, only the layers that differed between the two configurations were taken into account. In detail, the finishing layer, i.e., a dark asphalt shingles for the "standard roof" and a high reflectance tiles for the "cool roof", and a standard EPS insulation material were considered. Materials were selected in accordance with the technical properties modeled in the numerical analysis. Construction cost analysis was then performed using the European € cost for the above-mentioned materials based on typical local retail quotes.

According to the results of the previous thermal-energy analysis, the roof configurations selected for this analysis were:

- "cool roof" without thermal insulation layer
- "standard roof" with the thickest insulation layer (i.e., 0.25 m)
- "cool roof" with average insulation (i.e., 0.10 m)

The cost for asphalt shingles could be considered equal to around 8 €/m^2, while for cool tiles was higher and equal to about 15 €/m^2. The cost for EPS insulation ranged averagely from 6 €/m^2 for panels of 0.10 m thickness to 15 €/m^2 for panels up to 0.25 m thickness. Accordingly, the material cost for the three selected roof configurations (considering the sole materials that vary among the configurations) is reported in Table 7. Given the saving due to the elimination of the thermal insulation cost, the configuration with only the high reflectivity finishing was the cheapest among the three considered, followed by "cool roof" with average insulation and finally the dark roof with super-insulation. Therefore, the integrated design of roof thermal insulation level and solar reflectance capability could involve further cost savings in those boundary conditions where thermal insulation became negligible when a cool roof was installed.

Table 7. Comparison of construction cost for three example roof configurations.

Roof Configuration	Cost (€/m^2)
"cool roof" without thermal insulation	15
"standard roof" with 0.25 m thickness insulation	23
"cool roof" with 0.10 m thickness insulation	21

4. Discussion

The outcomes of the above reported analyses demonstrate how the annual thermal-energy performance of the roof in a standard small office building was significantly affected by the variation

of roof solar reflectance, while roof thermal insulation level was important only in extreme climate conditions, especially cold climates. Accordingly, when coupling the optimum design of roof solar reflectance and thermal insulation capability, the role of the second one in minimizing building annual HVAC energy consumption was negligible in the majority of considered climate zones, involving further savings in terms of construction costs. In fact, the cooling load was predominant in almost all the considered climate conditions, due to building end-use, i.e., office building, which was characterized by high internal gains. Therefore, the heating load was dampened down, while the cooling load became predominant also in cool and mild climate contexts. Nevertheless, in the coldest zones, a substantial insulating layer was required to limit the still significant heating energy losses.

In detail, in the "standard roof" scenario, which was characterized by higher external heat gains with respect to the "cool roof" due to the higher solar absorptance, roof thermal insulation provided significant benefits in terms of both cooling and heating energy savings. On the contrary, in the "cool roof" scenario, the high solar reflectance capability of the roof coating allowed the positive passive cooling effect able to minimize the cooling load. Although high thermal insulation level provided benefits in the cold season, the cooling load was even increased when thick insulating layers were implemented in hot and mild climate zones, since it did not allow the dissipation of internal heat gains. Therefore, when "cool roof" was applied over the building, the effect of thermal insulation was not required in these climate contexts, since in office buildings the cooling demand was generally predominant in the annual energy balance. Consistent results were obtained in an existing experimental and numerical study carried out in extreme hot weather conditions [19], where the difference in roof thermal energy performance with and without thermal insulation was found to be negligible.

Relevant findings are obtained, in particular, for mild and temperate climate zones, characterized by hot/warm summer and mild/cold winter. Accordingly, the expected optimum roof configuration, i.e., combination of roof solar reflectance capability and thermal insulation level, would involve a cool roof, which minimizes the cooling energy consumption, and maximum available thermal insulating layer thickness, which minimizes the heating energy consumption. Nevertheless, due to the above-mentioned phenomena and characteristics of the case study building typology, the optimum configuration was characterized by maximum solar reflectance and minimum thermal insulation, i.e., non-insulated cool roof. An existing experimental study evaluating the thermal-energy behavior of Nearly Zero Energy Buildings [17], confirmed the inverse relationship between the two characteristics of building roof considered, namely thermal resistance and external solar reflectance.

5. Conclusions and Future Developments

In the present study, a replicable method was implemented for optimizing the combined design of roof solar reflectance capability and roof thermal insulation level as passive strategy for building annual energy efficiency in different climate contexts worldwide. In this view, dynamic thermal-energy simulation was coupled with optimization analysis with the aim to minimize building annual HVAC energy requirement by optimizing the roof configuration. To characterize the roof configuration, two key parameters affecting building roof energy performance were taken into account, i.e., solar reflectance of the external coating and thermal insulation layer thickness. Moreover, to the aim of the work, the focus was on the application for a standard small office building.

The first relevant result was that "cool roof" optimized the annual HVAC energy consumption of the case study building in almost all considered climate conditions, except the two coldest zones. Moreover, between the two considered characteristics, building energy performance was more sensitive to roof solar reflectance variation. Nevertheless, when a low reflectance "standard roof" was implemented, roof thermal insulation variation significantly affected the building energy performance. Accordingly, when designing the roof, thermal insulation level should be selected by considering not only climate conditions but also roof coating thermo-optical characteristics. In general, when considering the combined design of roof solar reflectance capability and thermal insulation level, the optimum configuration could be differentiated in four classes according to the climate conditions.

In mild-warm climate zones, the optimum configuration was characterized by high passive cooling, i.e., ρ_{solar} equal to 0.8, and no insulating layer, i.e., $thickness_{ins}$ equal to 0.00 m. In mild-cold climate zones, the optimum configuration still involved a "cool roof", but coupled with high thermal insulation, i.e., $thickness_{ins}$ up to 0.25 m. In hot climate zones, the optimum configuration was again characterized by a "cool roof", but coupled with medium/low insulating layer thickness, i.e., $thickness_{ins}$ between 0.03 and 0.11 m, to limit the high thermal energy gains through the roof. Finally, in cold climate zones, the optimum configuration involved medium/low solar reflectance capability and high thermal insulation, i.e., $thickness_{ins}$ up to 0.25 m, to limit the significant thermal energy losses through the roof and help the additional thermal gains. Additionally, this optimized integrated design of roof configuration could potentially generate further cost savings in those climate zones where thermal insulation thickness can be reduced or neglected when a cool roof is installed.

Although the present study referred to limited cities, the selected climate zones represent a wide variety of climate conditions worldwide. Therefore, general indications were provided for building designers working in several climate contexts. Furthermore, the same procedure of analysis was easily reproducible for other climate zones. In addition, the outcomes stress how not just climate conditions, yet also further boundary conditions, namely end-use and envelope coating thermal and optical characteristics, have to be taken into account simultaneously when targeting building thermal-energy performance. Accordingly, future developments of this work could investigate the economic and life-cycle benefits associated to the coupled design of roof solar reflectance and thermal insulation. Furthermore, this promising multivariable optimization methodology could be implemented to study the influence of further relevant building boundary conditions in the optimum roof configuration, e.g., end-use, occupancy, type of operating system, etc. The final goal is to develop guidelines for the efficient implementation of cool roofs worldwide when varying the climate context and the other significant building boundary conditions.

Author Contributions: Conceptualization, C.P., A.L.P., M.S., A.G., and L.F.C.; methodology, C.P., M.S., and A.G.; Software, C.P. and M.S.; formal analysis, C.P. and M.S.; investigation, C.P., A.L.P., and M.S.; resources, A.L.P., F.C. and L.F.C.; data curation, C.P., M.S., and A.G.; writing-original draft preparation, C.P.; writing-review and editing, A.L.P., M.S., A.G., and L.F.C.; visualization, C.P., A.L.P., M.S., A.G., F.C., and L.F.C.; supervision, L.F.C. and F.C.; project administration, L.F.C. and F.C.; funding acquisition, L.F.C. and F.C.

Funding: The work was partially funded by the Spanish government (RTI2018-093849-B-C31). This work was partially supported by ICREA under the ICREA Academia programme. Dr. Alvaro de Gracia has received funding from the European Union's Horizon 2020 research and innovation programme under the Marie Sklodowska-Curie grant agreement No 712949 (TECNIOspring PLUS) and from the Agency for Business Competitiveness of the Government of Catalonia. This publication has emanated from research supported (in part) by Science Foundation Ireland (SFI) under the SFI Strategic Partnership Programme Grant Number SFI/15/SPP/E3125. The opinions, findings and conclusions or recommendations expressed in this material are those of the authors and do not necessarily reflect the views of the Science Foundation Ireland.

Acknowledgments: A previous contribution within this research study was published in the proceedings of international solar energy society (ISES) joint conference "ISES Solar World Congress 2017 and the international energy agency (IEA) solar heating and cooling (SHC) International Conference on Solar Heating and Cooling for Buildings and Industry 2017". The first author's acknowledgments are due to Regione Umbria and Department of Engineering at University of Perugia for supporting the project "SMEET-WELL: SMart building managEment for Energy saving meets WELLbeing". The authors from the University of Lleida would like to thank the Catalan Government for the quality accreditation given to their research group (2017 SGR 1537). GREiA is a certified agent TECNIO in the category of technology developers from the Government of Catalonia. The author from University College Dublin acknowledges the financial support provided by the Energy Systems Integration Partnership Programme (ESIPP), which is financially supported by Science Foundation Ireland.

Conflicts of Interest: The authors declare no conflict of interest.

Nomenclature

ρ_{solar}	Roof coating solar reflectance (-)
$thickness_{ins}$	Roof thermal insulation layer thickness (m)
U-value	Thermal transmittance (W/m^2·K)
HDD	Heating Degree Days (-)
CDD	Cooling Degree Days (-)
"standard roof"	Roof scenario characterized by ρ_{solar} equal to 0.3 and $thickness_{ins}$ according to the HDD of the climate zone
"cool roof"	Roof scenario characterized by ρ_{solar} equal to 0.8
f	User-defined objective function in the optimization analysis
x^i	i-th independent variable in the optimization analysis
l^i	Lower bound of the set of possible values for the i-th independent variable in the optimization analysis
u^i	Upper bound of the set of possible values for the i-th independent variable in the optimization analysis
E_{total}	Building annual HVAC energy consumption (kWh)
ΔE	Building annual HVAC energy consumption difference between the considered roof scenario and the "standard roof" scenario (kWh)

References

1. European Commission Energy Efficiency in Buildings. Available online: https://ec.europa.eu/energy/en/topics/energy-efficiency/buildings (accessed on 11 January 2018).
2. Santamouris, M. Innovating to zero the building sector in Europe: Minimising the energy consumption, eradication of the energy poverty and mitigating the local climate change. *Sol. Energy* **2016**, *128*, 61–94. [CrossRef]
3. Pisello, A.L. Experimental analysis of cool traditional solar shading systems for residential buildings. *Energies* **2015**, *8*, 2197–2210. [CrossRef]
4. Abuseif, M.; Gou, Z. A review of roofing methods: Construction features, heat reduction, payback period and climatic responsiveness. *Energies* **2018**, *11*, 3196. [CrossRef]
5. Levinson, R.; Akbari, H. Potential benefits of cool roofs on commercial buildings: Conserving energy, saving money, and reducing emission of greenhouse gases and air pollutants. *Energy Effic.* **2010**, *3*, 53–109. [CrossRef]
6. Pisello, A.L. State of the art on the development of cool coatings for buildings and cities. *Sol. Energy* **2017**, *144*, 660–680. [CrossRef]
7. Santamouris, M.; Ding, L.; Fiorito, F.; Oldfield, P.; Osmond, P.; Paolini, R.; Prasad, D.; Synnefa, A. Passive and active cooling for the outdoor built environment—Analysis and assessment of the cooling potential of mitigation technologies using performance data from 220 large scale projects. *Sol. Energy* **2017**, *154*, 14–33. [CrossRef]
8. Akbari, H.; Kolokotsa, D. Three decades of urban heat islands and mitigation technologies research. *Energy Build.* **2016**, *133*, 834–842. [CrossRef]
9. Santamouris, M. Regulating the damaged thermostat of the cities—Status, impacts and mitigation challenges. *Energy Build.* **2015**, *91*, 43–56. [CrossRef]
10. Hosseini, M.; Akbari, H. Heating energy penalties of cool roofs: The effect of snow accumulation on roofs. *Adv. Build. Energy Res.* **2014**, *8*, 1–13. [CrossRef]
11. Miller, W.; Crompton, G.; Bell, J. Analysis of cool roof coatings for residential demand side management in tropical Australia. *Energies* **2015**, *8*, 5303–5318. [CrossRef]
12. Hosseini, M.; Akbari, H. Effect of cool roofs on commercial buildings energy use in cold climates. *Energy Build.* **2016**, *114*, 143–155. [CrossRef]
13. Synnefa, A.; Santamouris, M.; Akbari, H. Estimating the effect of using cool coatings on energy loads and thermal comfort in residential buildings in various climatic conditions. *Energy Build.* **2007**, *39*, 1167–1174. [CrossRef]

14. Costanzo, V.; Evola, G.; Marletta, L. Cool roofs for passive cooling: performance in different climates and for different insulation levels in Italy. *Adv. Build. Energy Res.* **2013**, *7*, 155–169. [CrossRef]
15. Zinzi, M.; Carnielo, E.; Federici, A. Preliminary studies of a cool roofs' energy-rating system in Italy. *Adv. Build. Energy Res.* **2014**, *8*, 84–96. [CrossRef]
16. Lucero-Álvarez, J.; Martín-Domínguez, I.R. The effect of solar reflectance, infrared emissivity, and thermal insulation of roofs on the annual energy consumption of single-family households in México. *Indoor Built Environ.* **2019**, *28*, 17–33. [CrossRef]
17. Di Giuseppe, E.; D'Orazio, M. Assessment of the effectiveness of cool and green roofs for the mitigation of the Heat Island effect and for the improvement of thermal comfort in Nearly Zero Energy Building. *Archit. Sci. Rev.* **2015**, *58*, 134–143. [CrossRef]
18. Smith, G.B.; Aguilar, J.L.C.; Gentle, A.R.; Chen, D. Multi-parameter sensitivity analysis: A design methodology applied to energy efficiency in temperate climate houses. *Energy Build.* **2012**, *55*, 668–673. [CrossRef]
19. Radhi, H.; Sharples, S.; Taleb, H.; Fahmy, M. Will cool roofs improve the thermal performance of our built environment? A study assessing roof systems in Bahrain. *Energy Build.* **2017**, *135*, 324–337. [CrossRef]
20. Di Giuseppe, E.; Pergolini, M.; Stazi, F. Numerical assessment of the impact of roof reflectivity and building envelope thermal transmittance on the UHI effect. *Energy Procedia* **2017**, *134*, 404–413. [CrossRef]
21. Saffari, M.; de Gracia, A.; Fernández, C.; Cabeza, L.F. Simulation-based optimization of PCM melting temperature to improve the energy performance in buildings. *Appl. Energy* **2017**, *202*, 420–434. [CrossRef]
22. Dávi, G.A.; De Asiain, J.L.; Solano, J.; Caamaño-Martín, E.; Bedoya, C. Energy refurbishment of an office building with hybrid photovoltaic system and demand-side management. *Energies* **2017**, *10*, 1117. [CrossRef]
23. Kuang, J.; Zhang, C.; Li, F.; Sun, B. Dynamic optimization of combined cooling, heating, and power systems with energy storage units. *Energies* **2018**, *11*, 2288. [CrossRef]
24. Cascone, Y.; Capozzoli, A.; Perino, M. Optimisation analysis of PCM-enhanced opaque building envelope components for the energy retrofitting of office buildings in Mediterranean climates. *Appl. Energy* **2018**, *211*, 929–953. [CrossRef]
25. Gentle, A.R.; Aguilar, J.L.C.; Smith, G.B. Optimized cool roofs: Integrating albedo and thermal emittance with R-value. *Sol. Energy Mater. Sol. Cells* **2011**, *95*, 3207–3215. [CrossRef]
26. Aguilar, J.L.C.; Smith, G.B.; Gentle, A.R.; Chen, D. Optimum Integration of Albedo, Sub-Roof R-Value, and Phase Change Material for Cool Roofs. In Proceedings of the BS 2013: 13th Conference of the International Building Performance Simulation Association, Le Bourget Du Lac, France, 25–30 August 2013; pp. 1315–1321.
27. Farhan, S.A.; Shafiq, N.; Azizli, K.A.M.; Soon, F.K.; Jie, L.C. Optimization of residential roof design using system dynamics and building information modeling. In Proceedings of the Engineering Challenges for Sustainable Future, Proceedings of the 3rd International Conference on Civil, offshore and Environmental Engineering, Kuala Lumpur, Malaysia, 15–17 August 2016; pp. 193–198.
28. Arumugam, R.S.; Garg, V.; Ram, V.V.; Bhatia, A. Optimizing roof insulation for roofs with high albedo coating and radiant barriers in India. *J. Build. Eng.* **2015**, *2*, 52–58. [CrossRef]
29. Ramamurthy, P.; Sun, T.; Rule, K.; Bou-Zeid, E. The joint influence of albedo and insulation on roof performance: An observational study. *Energy Build.* **2015**, *93*, 249–258. [CrossRef]
30. Ramamurthy, P.; Sun, T.; Rule, K.; Bou-Zeid, E. The joint influence of albedo and insulation on roof performance: A modeling study. *Energy Build.* **2015**, *102*, 317–327. [CrossRef]
31. Saafi, K.; Daouas, N. A life-cycle cost analysis for an optimum combination of cool coating and thermal insulation of residential building roofs in Tunisia. *Energy* **2018**, *152*, 925–938. [CrossRef]
32. Piselli, C.; Saffari, M.; de Gracia, A.; Pisello, A.L.; Cotana, F.; Cabeza, L.F. Optimization of roof solar reflectance under different climate conditions, occupancy, building configuration and energy systems. *Energy Build.* **2017**, *151*, 81–97. [CrossRef]
33. Saffari, M.; Piselli, C.; de Gracia, A.; Pisello, A.L.; Cotana, F.; Cabeza, L.F. Thermal stress reduction in cool roof membranes using phase change materials (PCM). *Energy Build.* **2018**, *158*, 1097–1105. [CrossRef]
34. Piselli, C.; Pisello, A.L.; de Gracia, A.; Saffari, M.; Cotana, F.; Cabeza, L.F. Optimization of Coupled Building Roof Solar Reflectance and Thermal Insulation Level for Annual Energy Saving Under Different Climate Zones. In *SWC 2017/SHC 2017 /ISES Conference Proceedings*; International Solar Energy Society: Freiburg im Breisgau, Germany, 2017.

35. Crawley, D.B.; Pedersen, C.O.; Lawrie, L.K.; Winkelmann, F.C. Energy plus: Energy simulation program. *ASHRAE J.* **2000**, *42*, 49–56.
36. Wetter, M. Design Optimization with GenOpt. *Build. Energy Simul. User News* **2000**, *21*, 19–28.
37. Pisello, A.L.; Castaldo, V.L.; Piselli, C.; Fabiani, C.; Cotana, F. Thermal performance of coupled cool roof and cool façade: Experimental monitoring and analytical optimization procedure. *Energy Build.* **2017**, *157*, 35–52. [CrossRef]
38. ASHRAE. *ANSI/ASHRAE/IES ASHRAE Standard 90.1-2016—Energy Standard for Buildings Except Low-Rise Residential Buildings*; ASHRAE: Atlanta, GA, USA, 2016.
39. Crawley, D.B.; Lawrie, L.K.; Winkelmann, F.C.; Buhl, W.F.; Huang, Y.J.; Pedersen, C.O.; Strand, R.K.; Liesen, R.J.; Fisher, D.E.; Witte, M.J.; et al. EnergyPlus: Creating a new-generation building energy simulation program. *Energy Build.* **2001**, *33*, 319–331. [CrossRef]
40. Crawley, D.B.; Hand, J.W.; Kummert, M.; Griffith, B.T. Contrasting the capabilities of building energy performance simulation programs. *Build. Environ.* **2008**, *43*, 661–673. [CrossRef]
41. Perez, R.; Ineichen, P.; Seals, R.; Michalsky, J.; Stewart, R. Modeling daylight availability and irradiance components from direct and global irradiance. *Sol. Energy* **1990**, *44*, 271–289. [CrossRef]
42. Perez, R.R.; Ineichen, P.; Maxwell, E.L.; Seals, R.D.; Zelenka, A. Dynamic global-to-direct irradiance conversion models. *ASHRAE Trans.* **1992**, *98*, 354–369.
43. U.S. Department of Energy (DOE). *EnergyPlus Engineering Reference: The Reference to EnergyPlus Calculations*; Lawrence Berkeley National Laboratory: Alameda County, CA, USA, 2016; p. 1444.
44. Baños, R.; Manzano-Agugliaro, F.; Montoya, F.G.; Gil, C.; Alcayde, A.; Gómez, J. Optimization methods applied to renewable and sustainable energy: A review. *Renew. Sustain. Energy Rev.* **2011**, *15*, 1753–1766. [CrossRef]
45. Bamdad, K.; Cholette, M.E.; Guan, L.; Bell, J. Building energy optimisation under uncertainty using ACOMV algorithm. *Energy Build.* **2018**, *167*, 322–333. [CrossRef]
46. Prada, A.; Gasparella, A.; Baggio, P. On the performance of meta-models in building design optimization. *Appl. Energy* **2018**, *225*, 814–826. [CrossRef]
47. Sembroiz, D.; Careglio, D.; Ricciardi, S.; Fiore, U. Planning and operational energy optimization solutions for smart buildings. *Inf. Sci. (NY)* **2019**, *476*, 439–452. [CrossRef]
48. Lewis, R.M.; Torczon, V.; Trosset, M.W. Direct search methods: then and now. *J. Comput. Appl. Math.* **2000**, *124*, 191–207. [CrossRef]
49. Evins, R. A review of computational optimisation methods applied to sustainable building design. *Renew. Sustain. Energy Rev.* **2013**, *22*, 230–245. [CrossRef]
50. Hooke, R.; Jeeves, T.A. Direct Search' Solution of Numerical and Statistical Problems. *J. ACM* **1961**, *8*, 212–229. [CrossRef]
51. Wetter, M. *GenOpt(R) Generic Optimization Program User Manual Version 3.1.1*; Lawrence Berkeley National Laboratory: Berkeley, CA, USA, 29 March 2016.
52. Kottek, M.; Grieser, J.; Beck, C.; Rudolf, B.; Rubel, F. World map of the Köppen-Geiger climate classification updated. *Meteorol. Z.* **2006**, *15*, 259–263. [CrossRef]
53. Peel, M.C.; Finlayson, B.L.; McMahon, T.A. *Updated World Map of the Köppen-Geiger Climate Classification*; European Geosciences Union: Munich, Germany, 2007.
54. U.S. Department of Energy's (DOE) Building Technologies Office (BTO) EnergyPlus Weather Data. Available online: https://energyplus.net/weather (accessed on 12 December 2016).
55. Energy.gov. Office of Energy Efficiency & Renewable Energy Commercial Reference Buildings. Available online: https://energy.gov/eere/buildings/commercial-reference-buildings (accessed on 11 January 2018).
56. Winiarski, D.; Halverson, M.; Jiang, W. *PNNL's CBECS Study. Analysis of Building Envelope Construction in 2003 CBECS Buildings*; Pacific Northwest National Laboratory: Benton County, DC, USA, 2007.
57. Repubblica Italiana Ministero dello Sviluppo Economico. *Decreto Interministeriale 26 Giugno 2015 Applicazione Delle Metodologie di Calcolo Delle Prestazioni Energetiche e Definizione Delle Prescrizioni e Dei Requisiti Minimi Degli Edifici (In Italian)*; Ministero dello Sviluppo Economico: Rome, Italy, 2015.
58. Winiarski, D.; Jiang, W.; Halverson, M. *PNNL's CBECS Study. Review of Preand Post-1980 Buildings in CBECS–HVAC Equipment*, 2006.

59. EN 15251, CS. *Indoor Environmental Input Parameters for Design and Assessment of Energy Performance of Buildings Addressing Indoor Air Quality, Thermal Environment, Lighting and Acoustics*; European Committee for Standardization: Brussels, Belgium, 2007.
60. Allesina, G.; Mussatti, E.; Ferrari, F.; Muscio, A. A calibration methodology for building dynamic models based on data collected through survey and billings. *Energy Build.* **2018**, *158*, 406–416. [CrossRef]